An Acad Bras Cienc (2023) 95(2): e20201518 DOI 10.1590/0001-3765202320201518
Anais da Academia Brasileira de Ciências | *Annals of the Brazilian Academy of Sciences*
Printed ISSN 0001-3765 I Online ISSN 1678-2690
www.scielo.br/aabc | www.fb.com/aabcjournal

CHEMICAL SCIENCES

Impact assessment of synthesis parameter stirring speed in final physicochemical properties of PU microcapsules incorporated into epoxy matrixes

ALEXANDRE ESTÊVÃO CARRARA, VINÍCIUS HENRIQUE DE S. RODRIGUES, RITA DE CÁSSIA L. DUTRA & JORGE CARLOS N. DUTRA

Abstract: A considerable number of papers have been published to assess self-healing capacity of several materials, as well as several applications in different areas. However, the impact assessment of changing synthesis parameters of microcapsules, hollow fibers or microvascular systems in its final physicochemical properties are still an emerging research field. This current paper presents a synthesis process of PU microcapsules containing TDI as core agent and the characterization of microcapsules physicochemical properties. During the synthesis, the reaction parameter stirring speed was changed to assess the impact that this parameter has in the final microcapsules' physicochemical properties. Microcapsules were characterized by FT-IR, TGA and image analysis (OM and SEM). Additionally, microcapsules were incorporated to an epoxy matrix (5% weight/weight) to assess the impact in the final physicochemical and mechanical matrix properties. Epoxy-based test specimens were also obtained within aramid and silica, which are traditional reinforcing loads in rubber synthesis. Final mechanical properties of matrixes within aramid and silica were compared to the properties of matrixes within microcapsules to determine what kind of behavior the microcapsules have when incorporated to epoxy matrixes.

Key words: Polyurethane, microencapsulation, polymers, stirring speed, self-healing.

INTRODUCTION

Self-healing polymers represent a recent technological improvement in applications that require structural security, reliability, and durability, once those materials have the ability to self-repair chemically and physically in microscopic scale after exposed to a mechanical/thermal or any kind of stress that drives to structural damages or fissures (Cho et al. 2006).

The motivation to develop self-healing materials are the living organisms that have the capacity to self-regenerate, e.g., blood coagulation or fractured bones recovery. Plants and sea animals also have the capacity of self-regeneration (Ghosh 2009, Lee et al. 2018).

The basic principle of self-healing is the formation of a mobile phase triggered by damages or fissures (Hager et al. 2010). Mobile phase is composed by healing agent. Usually, the healing agent is stored into microcapsules, hollow fibers or microvascular systems (Dry et al. 1992, Brown et al. 2002, Wu et al. 2008, Wang et al. 2015).

White et al. (2001) have performed the first self-healing microcapsule experiment with the microencapsulation of dicyclopentadiene (DCPD) using urea-formaldehyde as

microcapsule shell. Healing agent DCPD is released after cracking of microcapsule. These microcapsules were incorporated into an epoxy matrix, simultaneously to Grubb's catalyst, which major drawback is its high cost. The polymerization of the healing agent is triggered by the contact with Grubb's catalyst. The recovery of 75% in toughness of epoxy matrix was achieved through fracture experiments, proving the healing efficiency of this system. The inconvenience of the high cost associated led to non-catalytic process studies using liquid hexamethylene diisocyanate (HDI) (Huang et al. 2011) and liquid isophorone diisocyanate (IPDI) (Alizadegan et al. 2017, Yang et al. 2008).

A considerable number of papers have been published to assess self-healing capacity of several materials, as well as several applications in different areas (Lee et al. 2018, Wu et al. 2016, Zechel et al. 2017, Chung et al. 2017, Yu et al. 2018, Yang et al. 2019, Zhao et al. 2019, Rodrigues et al. 2019). However, the impact assessment of changing synthesis parameters of microcapsules, hollow fibers or microvascular systems in its final physical and chemical properties are still an emerging research field. This impact assessment is essential to define optimized synthesis conditions, as well as application limits.

A recent paper (Lee et al. 2018) has studied the effect of changing the composition of surfactant system in the synthesis process of polyurethane (PU) within encapsulated diisocyanate microcapsules for application in poly (ether) sulfone membranes used in water treatment stations. In this study, the amount of auxiliary surfactant dodecyltrimethylammonium bromide (DTAB) was gradually increased during the synthesis of microcapsules.

Several analytical techniques, as Scanning Electron Microscopy (SEM), Fourier Transform Infrared Spectroscopy (FT-IR), Thermogravimetric Analysis (TGA) and Differential Scanning Calorimetry (DSC) were applied to characterize the final properties of resultant microcapsules. Lee et al. (2018) have concluded that as the amount of the auxiliary surfactant increases, the microcapsules became denser and more robust. On the other hand, the self-healing capacity was lower as higher the amount of auxiliary surfactant was.

In the present paper, PU microcapsules were synthesized by emulsion polymerization through the reaction between 1,4-butanediol and MDI to form PU shell and TDI was encapsulated into microcapsules as core agent (self-healing agent). Although both diisocyanates (MDI and TDI) has reactivity with 1,4-butanediol, the reaction of the MDI / 1,4-butanediol pair started at a lower temperature than the reaction of TDI / 1,4-butanediol pair, then TDI is preferably used as core agent than PU synthesis reagent (Rodrigues et al. 2019). The highest reactivity of MDI / 1,4-butanediol pair happens because the electrons of isocyanate group (NCO) have more availability to react in MDI than in TDI as TDI has the physical interference of electrons for methyl group ($-CH_3$) (Grunwald 1999).

This reaction was performed at constant temperature and five different stirring speed (250, 400, 600, 800, and 1000 RPM) were considered. It is expected to obtain higher microcapsules as lower the stirring speed is (Huang et al. 2011).

Several characterization techniques were applied to assess the impact that the parameter reaction stirring speed has in the final PU properties, to cite, FT-IR for chemical characterization, SEM for morphological and size characterization, Optical Microscopy (OM) for evaluation of microcapsules size distribution and TGA for characterization of thermal degradation profile.

Microcapsules were added into polymer matrix (5% w/w) and several physical, chemical,

and mechanical properties were assessed through tensile strength assay (to measure matrix rupture tension) and Shore D hardness (to measure matrix hardness).

The physical tests applied to epoxy-based test specimens containing aramid and silica had the goal to compare the physical influence of the addition of those materials to the addition of microcapsules into polymer matrix, since aramid and silica are reinforcement loads widely used in ablative thermal protections in aerospace industry.

Microcapsules sizes were inversely proportional to stirring speed. TDI encapsulation was satisfactory and thermal profile was not impacted by stirring speed change. Microcapsules had a behavior of filling loads when incorporated to epoxy matrix.

MATERIALS AND METHODS

Materials

All materials applied on this paper are commercially available. Isotek 5501 (MDI pre-polymer) and TDI were donated by Shimtek and used as received. The 1,4-butanediol 99% and 1,2-dichloroethane P.A were purchased from Sigma-Aldrich (Brazil). Polyvinyl alcohol (PVA), degree of hydrolysis 88%, with MW = 25,000 was purchased from Carvalhaes (Brazil). Epoxy resin, Ampreg 26 high Tg, was purchased from E-composites (Brazil). Aramid Fiber 3 mm, Technora Teijin, was donated by Instituto de Aeronáutica e Espaço (IAE - Brazil). Sílica powder, Zeosil 175 P, was manufactured by Solvay and donated by Tenneco (Brazil).

Synthesis of microcapsules

Synthesis of PU microcapsules follows an *in situ* polymerization in an oil-in-water emulsion system (Alizadegan et al. 2017, Haghayegh et al. 2016, Jones et al. 2015), in which diisocyanates (MDI and TDI) and diol (1,4-butanediol) need to be dispersed in a surfactant system to create an emulsion and then be dispersed in the oily phase (Alizadegan et al. 2018).

Firstly, polyvinyl alcohol (PVA) was dissolved in hot water (90°C) and mechanical stirring. This solution was cooled to room temperature at a stirring speed of 600 RPM for 30 minutes (Solution A). In parallel, a different solution of methyl diphenyl diisocyanate (MDI) pre-polymer and TDI diluted in 1,2-chloroethane was prepared under temperature of 60°C (Solution B). Solution A and B were mixed through different stirring speed (250, 400, 600, 800, and 1000 RPM) and controlled temperature (40°C). 1,4-butanediol was slowly added to these mixtures of solutions and the reaction parameters (stirring speed and temperature) was controlled by 60 minutes. Finally, the resulting microcapsules were filtered in a vacuum system and dried. Then, different samples of microcapsules were obtained at different stirring speeds. Synthesis process is summarized at Figure 1.

Microcapsules yield

The reaction yield for the encapsulation synthesis was calculated, considering TDI as the core agent. Huang et al. (2011) proposed the methodology applied to obtain its value.

$$yield\ (\%) = \frac{W_{cap}}{W_{prep} + W_{diol} + W_{iso}}\ x\ 100\%$$

Where W_{cap} is the mass of the microcapsules, $W_{pre\text{-}p}$ is the mass of the MDI prepolymer, W_{diol} is the mass of the 1,4-butanediol, and finally W_{iso} is the mass of the core agent.

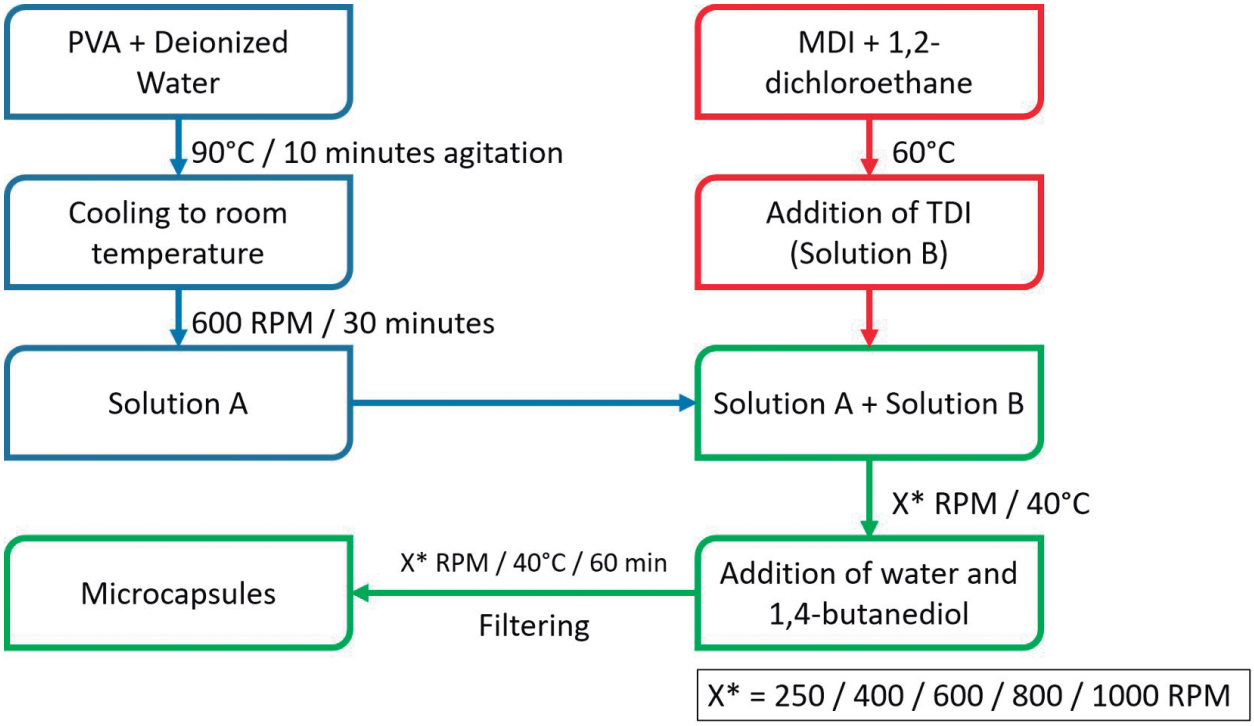

Figure 1. Summary of process synthesis.

Microcapsules characterization

The distribution profile size was determined by OM images using microscope Quimis Q730MIT applying image magnifications of 4x and 10x.

Microcapsules morphology were evaluated by SEM images using Tescan Mira 3 equipment, at variable pressure, after spraying the samples in an adhesive tape.

The diisocyanates, microcapsules, and polymer matrixes used to obtain the composites were analyzed as received by FT-IR using the Perkin Elmer Frontier spectrometer. The spectra were collected over the range 4000 to 400 cm^{-1} (MIR- mid infrared region), with a resolution of 4 cm^{-1} and gain 1, 20 scans, by universal attenuated total reflection (UATR) mode. At the first moment, the microcapsules were analyzed under 7 N contact to avoid its cracking and then 80 N (with and without previous trituration) was applied to stimulate the cracking and the consequent release of core agent TDI.

Thermal analysis was performed by TGA, using the model TGA / DTA 6200 SII EXSTAR 6000 equipment, in a temperature range between room temperature up to 500 °C, heating rate of 10 °C / min, in an inert atmosphere of Nitrogen (N_2).

Manufacturing of epoxy-based test specimens

The microcapsules containing TDI as core agent were individually incorporated into the epoxy matrix, at a ratio of 5 wt.%, and dispersed under manual shaking by using a glass rod (Lee et al. 2015, Li et al. 2013). After this step, the blend was transferred to a silicone template to cure under vacuum at room temperature. The stoichiometry applied to cure epoxy was 1:0.29 (epoxy resin / hardener).

Epoxy-based test specimens' characterization

Rupture tension was determined by tensile strength assay using dynamometer Zwick 1474 with controlled temperature (22° C) and humidity

(49%) per ASTM D638. A deformation rate of 1 mm/min was applied and the test stopped when specimens cracked. Shore D hardness was determined using a Durometer Zwick with controlled temperature (22°C) and humidity (49%) per ASTM D2240.

RESULTS AND DISCUSSION

Reaction yield calculation

The calculation of synthesis reaction yield was done for all the synthesis processes as described in item 'Synthesis of microcapsules' according to yield equation presented in item'Microcapsules yield'. Results are summarized in Table I.

Yield calculation allows the differentiation between synthesis processes. The synthesis adopting 800 RPM as stirring speed had the best yield (64.36%), while synthesis at 1000 RPM presented the worst yield (17.10%).

Results of reactions 1 to 4 present values considered acceptable by some authors. 70% of average yield (Huang et al. 2011, Alizadegan et al. 2017) and values closer to 50% (Li et al. 2013) were already reported. Reaction # 5, in opposite, presented a low yield reaction, demonstrating that synthesis reaction at 1000 RPM stirring speed has low potential of reproducibility and application.

Microcapsules characterization analysis

In this section are presented characterization results for the synthesized microcapsules through FT-IR, OM, SEM, and TGA analysis.

Fourier-Transform Infrared Spectroscopy - FT-IR

FT-IR technique was applied to characterize the formation of microcapsule PU shell structure in the reaction of 1,4-butanodiol / MDI pair. FT-IR was also considered to monitor TDI encapsulation. Figure 2 shows the expected chemical PU structure after microcapsules formation.

Microcapsules synthesized at different stirring speeds were analyzed through three conditions using UATR accessory. Figure 3 shows following spectra: (1) 7 N contact to avoid microcapsules cracking (black spectra); (2) 80 N contact to stimulate microcapsules cracking and the consequent TDI core agent release. In

Table I. Synthesis reaction yield results.

Reaction #	Stirring speed (RPM)	W_{cap} (g)	W_{MDI} (g)	W_{diol} (g)	W_{TDI} (g)	Yield (%)
1	250	21.13	7.38	7.65	22.99	55.58
2	400	22.03	7.38	7.65	22.99	57.94
3	600	16.33	7.38	7.65	22.99	42.96
4	800	24.47	7.38	7.65	22.99	64.36
5	1000	6.50	7.38	7.65	22.99	17.10

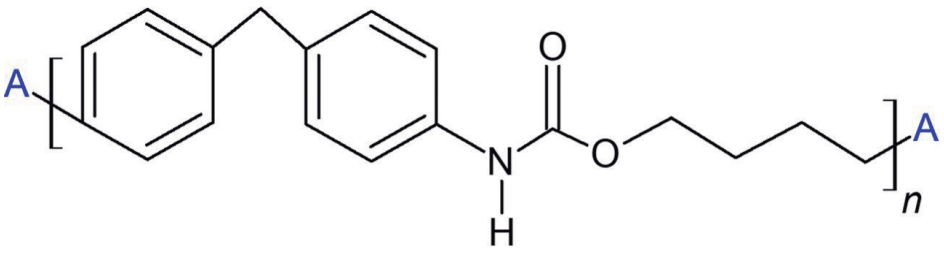

Figure 2. PU chemical structure resulting of reaction of 1,4-butanodiol and MDI.

this step is expected to see a more pronounced isocyanate band (NCO) (red spectra); (c) samples were pre-triturated before analysis with 80 N contact to stimulate TDI core agent releasing (green spectra). A more intense NCO band is expected in step C when compared to previous steps. Figure 3 shows all spectra collected in this analysis.

A characteristic isocyanate band (NCO) is observed at 2268 cm^{-1} in all spectra and its intensity is increasing as the microcapsule cracking is stimulated. Figure 3 (a) to (e) highlights the intensity band increase due to higher releasing of TDI core agent, which demonstrates that TDI was successfully encapsulated into PU shell, as already demonstrated by Rodrigues et al. (2019).

As all overlaid spectra have the same bands, the changing in stirring speed has no impact in the process of PU synthesis. Then, a single sample was chosen just to illustrate PU spectrum and its characteristic bands. Figure 4 illustrates the 7 N contact spectra for 250 RPM microcapsule sample.

Amine band (NH) was observed in 3279 cm^{-1}, C=O in 1588 cm^{-1}, aromatic C-C band in 1219 cm^{-1}, C-O-CO in 1065 cm^{-1}. Isocyanate aromatic band is also observed in 2266 cm^{-1} and 571 cm^{-1} (Hummel 2002), demonstrating that UATR was able to identify TDI agent core bands due to penetration in the surface samples. Data achieved are suitable to data reported in the literature (Rodrigues et al. 2019).

Optical Microscopy - OM

OM was applied to determine the profile size distribution of PU microcapsules. It is expected to have a correlation of microcapsules diameter and stirring speed, as reported by Huang et al. (2011). According to the authors, when higher the stirring speed applied in the synthesis reaction, lower the size of microcapsules, once the increase of stirring speed contributes to the formation of finer oil droplets due to stronger shear force and

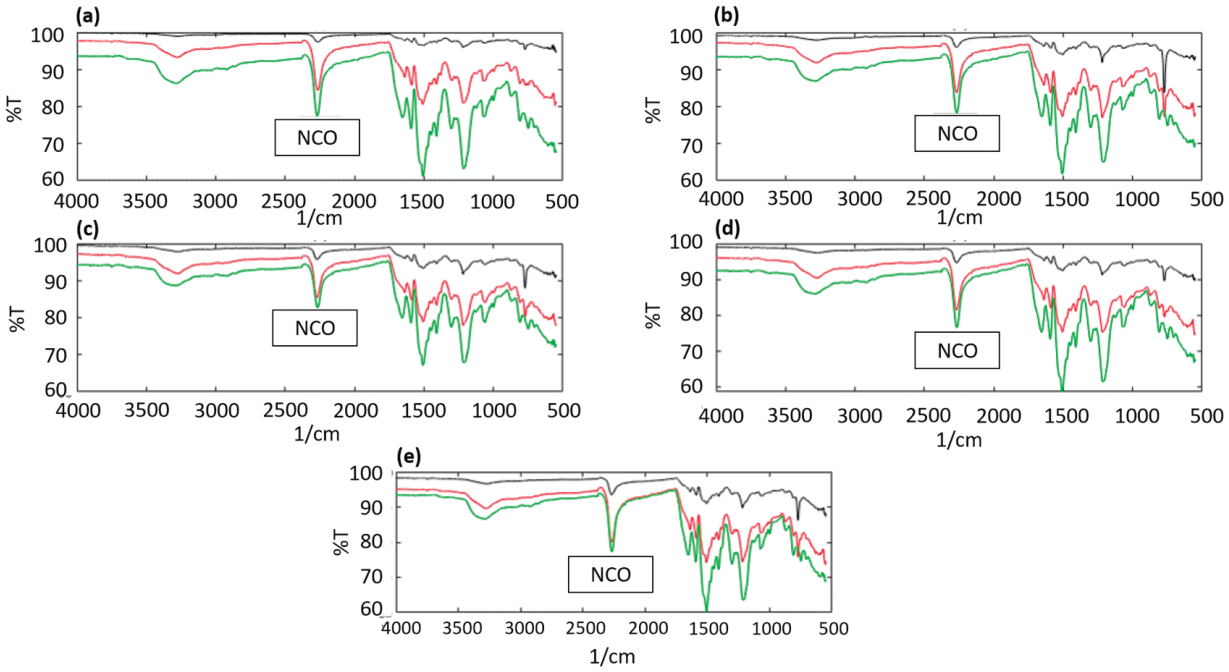

Figure 3. Overlaid FT-IR spectra. (a) 250 RPM sample; (b) 400 RPM sample; (c) 600 RPM sample; (d) 800 RPM sample; (e) 1000 RPM sample.

then the microcapsules is accordingly smaller. Faster agitation also contributes to produce a more uniform diameter distribution.

Microcapsules dimensions were determined through the measure of a minimal of 200 microcapsules for each condition synthesis and the values of frequency (f_i) and relative frequency (f_{ri}) were determined. Frequency corresponds to the number of microcapsules in a fixed size range, while relative frequency is the ratio between the number of microcapsules in a fixed size range (the frequency) and total number of microcapsules considering all the size ranges.

Figure 5 shows the graphs of profile size distribution for all the five conditions of synthesis.

The correlation between microcapsule size and stirring speed is clearly observed in Figure 5. At 250 RPM, the maximum frequencies are observed in the size range of 50 – 69.9 µm (22.5% of total population) and 70 – 89.9 µm (21.7%

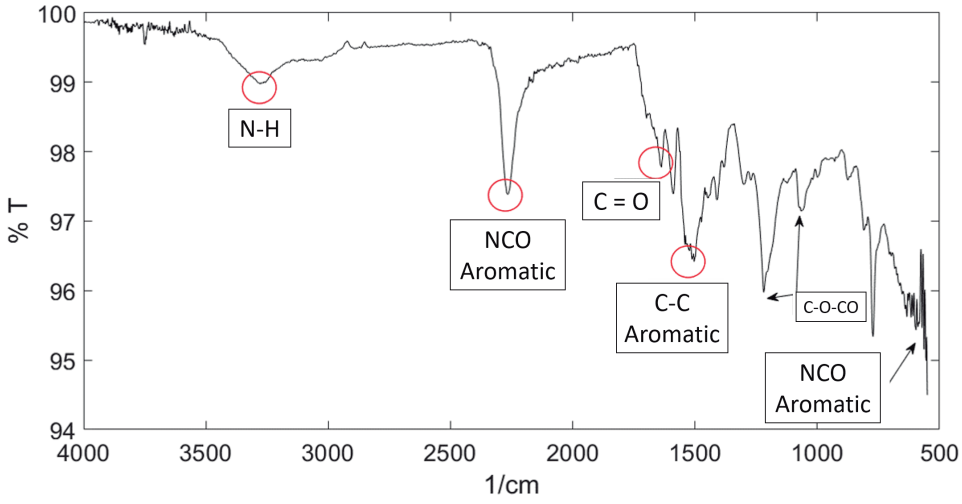

Figure 4. FT-IR spectrum for 250 RPM sample at 7 N contact.

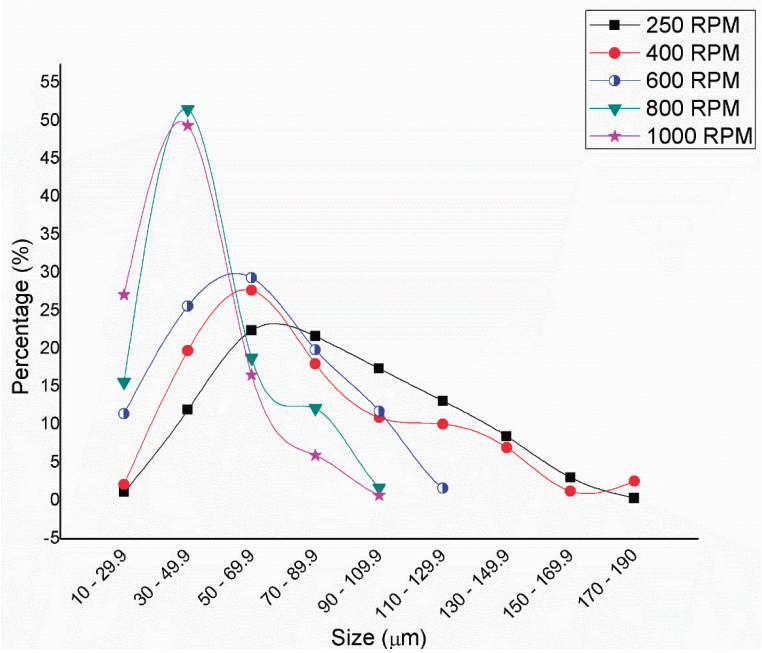

Figure 5. Overlaid size distribution profiles for PU microcapsules synthesis processes.

of total population), while at 1000 RPM the maximum frequency is achieved from 30 to 49.9 µm (49.9% of total population). The average size values were also determined to better clarify the difference between the conditions of synthesis. Table II summarizes those results.

Data reported in Table II reinforces the conclusion that microcapsules size is higher when the stirring speed is lower. The only deviation is the value of mode for 800 RPM sample set, which is lower than the correspondent one for 1000 RPM. This result, however, is not an unexpected result, once for both sample sets (800 and 1000 RPM) the most frequent size range is 30 – 49.9 µm.

Scanning Electron Microscopy - SEM

SEM analysis was applied to compare the morphology of microcapsules obtained for all synthesis processes, as well as to determine the thickness of PU microcapsules shell, to evaluate how stirring speed affect those parameters.

Figure 6 (a) to (d) shows individual cracked microcapsules obtained from synthesis processes of stirring speeds from 250 to 800 RPM to illustrate morphology, as well as the

Table II. Average microcapsules size values.

Stirring Speed (RPM)	Average (µm)	Mode (µm)	Median (µm)
250	86	63	83
400	78	56	70
600	60	54	58
800	46	33	41
1000	41	44	39

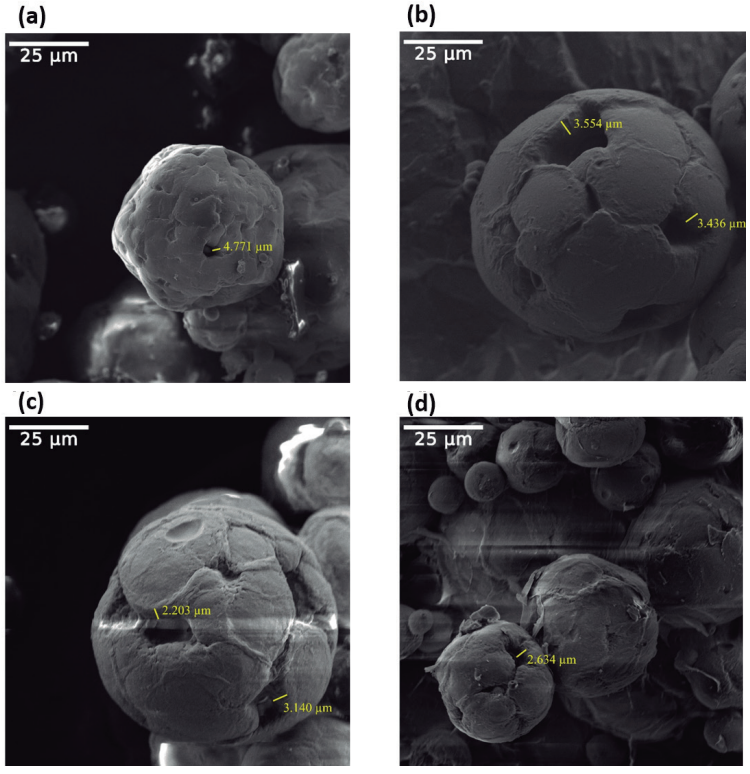

Figure 6. (a) Individual microcapsule synthesized at 250 RPM (1000x of magnification); (b) Individual microcapsule synthesized at 400 RPM (3000x of magnification); (c) Individual microcapsule synthesized at 600 RPM (3700x of magnification); (d) Individual microcapsule synthesized at 800 RPM (3000x of magnification).

shell thickness. It was not possible to identify an individual cracked microcapsule synthesized at 1000 RPM, possibly due to low reaction yield. Microcapsules formed by the five conditions have spherical profile and is observed a roughness in PU shell.

The thickness of individual microcapsules was measured through the image processing. For 250 RPM microcapsules, the thickness measured was around 4.8 µm. For 400 RPM microcapsule, two cracks were measured, within an average of 3.5 µm, as well for 600 RPM microcapsules, in which the average value was 2.7 µm. Finally, the value measured for 800 RPM microcapsules was around 2.6 µm. Thickness data are summarized at Table III.

This analysis shows a tendency of thickness decrease as the stirring speed increases, even analyzing just an individual microcapsule for each sample set. This could demonstrate that the microcapsule synthesized with 250 RPM stirring speed is the higher one, also with highest thickness. During the use of microcapsules as self-healing agents, this could mean that 250 RPM microcapsule is more resistant to crack than the other ones.

Thermogravimetric Analysis - TGA

Thermal degradation profile of microcapsules was achieved by TGA analysis. As showed by Figure 7, the similarity between degradation profiles is very high and there are no significant differences, demonstrating that the microcapsule size did not affect the thermal degradation profile and that the same PU material was synthesized for all the synthesis adopted.

Figure 8 shows the TGA derivative graphs (DTGA) to determine the temperature of maximum thermal degradation, reinforcing the similarity between all samples analyzed, although some differences were observed for the samples synthesized at higher stirring speed (600, 800 and 1000 RPM), as an additional peak was identified at 285°C, which may be derived from some secondary thermal reaction. For all samples, peak at 310°C was observed as main temperature of degradation.

Table III. Thickness microcapsules data.

Sample	250 RPM microcapsules	400 RPM microcapsules	600 RPM microcapsules	800 RPM microcapsules
Thickness (µm)	4.8	3.5	2.7	2.6

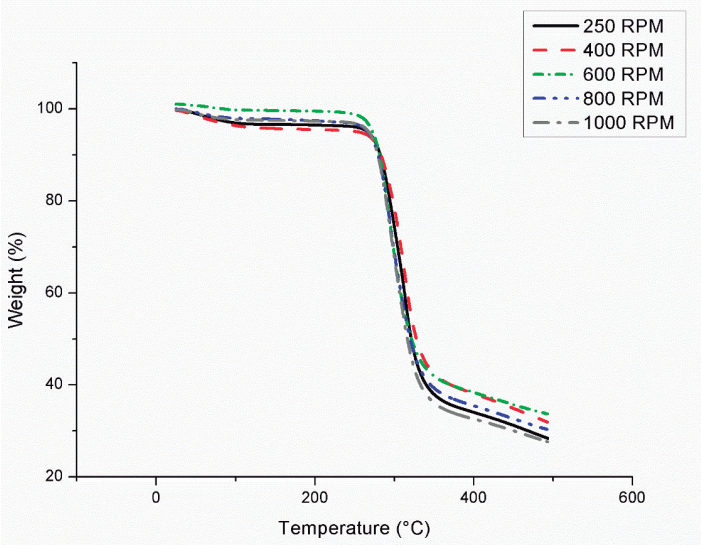

Figure 7. Comparative thermal degradation profiles of all microcapsules synthesized.

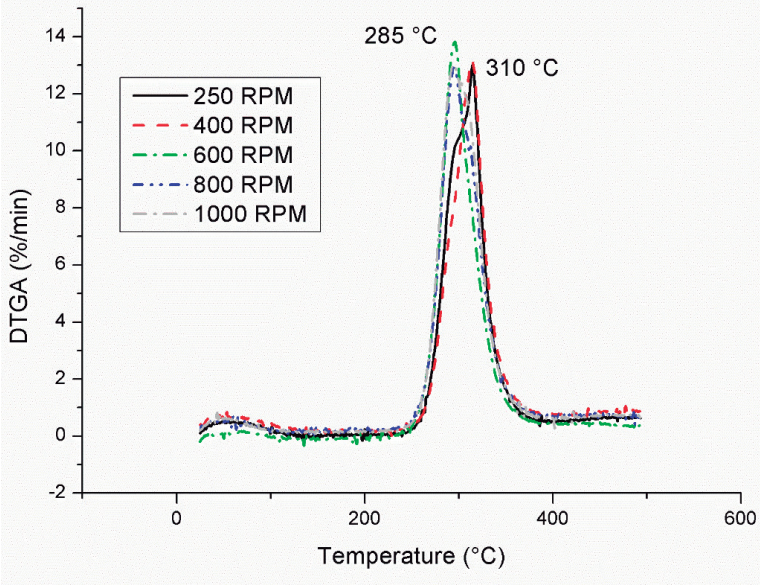

Figure 8. DTGA comparative graphs.

Epoxy-based specimens test characterization analysis

In this section are presented the results of characterization analysis for epoxy-based specimens test through tensile strength and shore D hardness. Non-charged epoxy-based specimens test was analyzed, as well as within PU microcapsules, aramid, and silica.

Rupture tension by tensile strength technique

Tensile strength assay was applied to evaluate the impact that the charge (PU microcapsules, aramid, and silica) has in the rupture tension of epoxy-based specimen test. Figure 9 summarizes results.

Through the results obtained, is evident that rupture tension has decreased in the specimens within microcapsules, which indicates that the mechanical properties are worse when comparing to the non-charged specimen. Brown et al. (2004), have predicted this behavior once microcapsules have the function of filling load to the polymer. The addition of silica and aramid, on the other hand, has the opposite effect, since the rupture tension has increased, reflecting in the improvement of mechanical properties.

This is an expected result, once silica is traditionally applied as reinforcement load to improve rubber properties and aramid is used for applications that require high impact resistance.

The characteristic of thermoset epoxy was not modified once no deformations were observed for any specimens.

Hardness by Shore D hardness technique

Shore D hardness assay was applied to evaluate the impact that the addition of different materials to epoxy resin has in the hardness value. Average values of five measures are summarized in Figure 10.

Results demonstrated that the addition of PU microcapsules to epoxy matrix decreases hardness of non-charged matrix for all the samples of microcapsules considered in this study. The addition of microcapsules negatively affects mechanical properties of polymer matrixes, as microcapsules have the function of filling load to the polymer matrix (Brown et al. 2004). Same influence was observed in rupture tension results, as the addition of microcapsules resulted in a decrease of mechanical property.

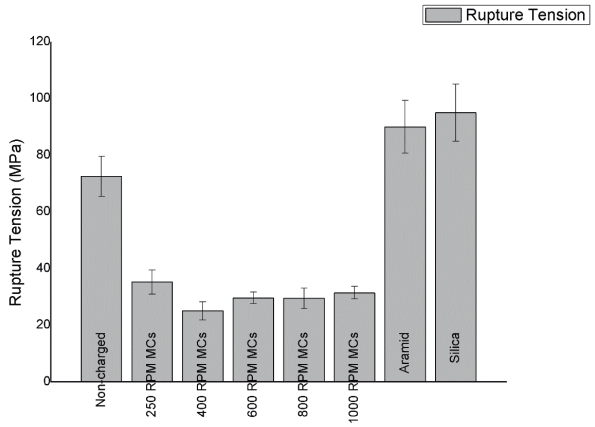

Figure 9. Rupture tension determination.

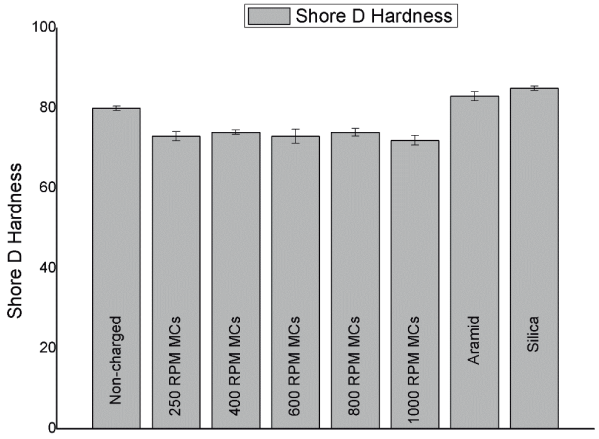

Figure 10. Average of Shore D hardness determination.

The addition of silica and aramid results in the opposite effect, as both materials are reinforcing load and had increased the value of composite hardness, probably due to better compatibility to the matrix (Cao et al. 2013, Kralevich et al. 1998).

TRENDS

The development of new self-healing materials for different segments of industry and research fields are considerably increasing in the recent past years with the study of different microcapsules, self-healing agents, catalysts, and application matrixes. Most of the published papers are focused to demonstrate self-healing capacity, but the assessment of the synthesis parameters change in the final physicochemical properties of microcapsules, hollow fibers or microvascular systems are still an emergency research field. The use of several analytical techniques to characterize the final properties of those materials are essential to determine the ranges of application (e.g., optimal temperature conditions) and to state proper conditions of synthesis to improve yield reaction and laboratory security.

CONCLUSION

The process to optimize the reaction to synthesize PU microcapsules containing TDI through *in situ* polymerization by emulsion and stirring speed variation (250, 400, 600, 800, and 1000 RPM), allows to conclude that the increase of stirring speed is inversely proportional to microcapsules size and shell thickness. Reactions from 250 to 800 RPM had acceptable yield values.

The application of chemical, morphological, and thermal characterization analysis allows to confirm TDI encapsulation, morphological aspect of PU shell (spherical and rough appearance), size distribution profile, as well as thermal degradation profile (not impacted by microcapsules dimensions).

Microcapsules were successfully dispersed into epoxy resin and no interference was observed in the composite cure. Tensile strength and Shore D hardness showed that microcapsules act as filling loads, as tensile strength was reduced in 58% and hardness in 10% in the composites after microcapsules incorporation. The opposite effect was observed when silica and aramid were incorporated to epoxy matrix, which is coherent to the application that those materials have as reinforcement loads.

Acknowledgments

The authors would like to thank the Divisão de Propulsão (APR) and Materiais (AMR), two Brazilian Chemistry Divisions of IAE, for enabling the development of this paper, making the infrastructure/equipment available for conducting the tests, and supporting their teams in all phases of the research, and we also thank the company Shimtek for the donation of prepolymer MDI and TDI and the Instituto de Aeronáutica e Espaço (IAE - Brazil) for the donation of Aramid 3 mm Technora Teijin. This study was partially supported by Conselho Nacional de Desenvolvimento Científico e Tecnológico (CNPq) Finance Code 301626/2022-7.

REFERENCES

ALIZADEGAN F, MIRABEDINI SM, PAZOKIFARD S, GOHARSHENAS S & FARNOOD R. 2018. Improving self-healing performance of polyurethane coatings using PU microcapsules containing bulky-IPDI-BA and nano-clay. Prog Org Coat 123: 350-361.

ALIZADEGAN F, PAZOKIFARD S, MIRABEDINI SM, DANAEI M & FARNOOD R. 2017. Polyurethane-based microcapsules containing reactive isocyanate compounds: study on preparation procedure and solvent replacement. Colloids Surf 529: 750-759.

BROWN EN, SOTTOS NR & WHITE SR. 2022. Fracture testing of a self-healing polymer composite. Exp Mech 42: 372-379.

BROWN EN, WHITE SR & SOTTOS NR, 2004. Microcapsule induced toughening in a self-healing polymer composite. J Mater Sci 39: 1703-1710.

CAO K, SIERPERMANN CP, YANG M, WAAS AM, KOTOV NA, THOULESS MD & ARRUDA EM. 2013. Reactive Aramid Nanostructures as high-performance polymeric building blocks for advanced composites. Adv Funct Mater 23: 2072-2080.

CHO SH, ANDERSSON HM, WHITE SR, SOTTOS NR & BRAUN PV. 2006. Polydimethylsiloxane-based self-healing materials. Adv Mater 18: 997-1000.

CHUNG US, MIN JH, LEE PC & KOH WG. 2017. Polyurethane matrix incorporating PDMS-based self-healing with enhanced mechanical and thermal stability. Colloids Surf 518: 173-180.

DRY CM & SOTTOS NR. 1992. Passive smart self-repair in polymer matrix composite materials. In: CONFERENCE ON RECENTE ADVANCES IN ADAPTIVE AND SENSORY MATERIALS AND THEIR APPLICATIONS. Albuquerque, NM. Proceedings [...]. Bellingham, WA, p. 438-444.

GHOSH SK. 2009. Self-healing materials: fundamentals, design, strategies, and applications. Weinheim: Willey-VCH Verlag, 291 p.

GRUNWALD D. 1999. New analytical methods as tools for the determination of resin properties new analytical methods as tools for the determination of resin properties. In: EUROPEAN WOOD-BASED PANEL SYMPOSIUM. Hannover. *Proceedings* [...]. Munich: Fraunhofer-Gesellschaft, 9 p.

HAGER MD, GREIL P, LEYENS C, ZWAAG S & SCHUBERT US. 2010. Self-healing materials. Adv Mater 22: 5424-5430.

HAGHAYEGH M, MIRABEDIN SM & YEGANEH H. 2016. Microcapsules containing multi-functional reactive isocyanate-terminated polyurethane prepolymer as a healing agent. Part 1: synthesis and optimization of reaction conditions. J Mater Sci 51: 3056-3068.

HUANG M & YANG J. 2011. Facile microencapsulation of HDI for self-healing anticorrosion coatings. J Mater Chem 21: 11123-11130.

HUMMEL DO. 2002. Atlas of plastics additives: analysis by spectrometric methods. Berlin: Springer-Verlag 1: 537 p.

JONES AR, WATKINS CA, WHITE SR & SOTTOS NR. 2015. Self-healing thermoplastic-toughened epoxy. Polymer 74: 254-261.

KRALEVICH ML & KOENIG JL. 1998. FTIR analysis of silica-filled natural rubber. Rubber Chem Technol 71: 300-309.

LEE J, BHATTACHARYYA D, ZHANG MQ & YUAN YC. 2015. Mechanical properties of a self-healing fiber reinforced epoxy composites. Compos B Eng 78: 515-519.

LEE J, PARK SJ, PARK CS, KWON OS, CHUNG SY, SHIM J, LEE CS & BAE J. 2018. Effect of a surfactant in microcapsule synthesis on self-healing behavior of capsule embedded polymeric films. Polymers 10: 1-13.

LI Q, SIDDARAMAIAH, KIM NH, HUI D & LEE JH. Effects of dual component microcapsules of resin and curing agent on the self-healing efficiency of epoxy. Compos B 55: 79-85.

RODRIGUES VHS, CARRARA AE, ROSSI SS, SILVA LM, DUTRA RCL & DUTRA JCN. 2019. Synthesis, characterization and qualitative assessment of self-healing capacity of PU microcapsules containing TDI and IPDI as a core agent. Mater Today Commun 21: 100698.

WANG Y, PHAM DT & JI C. 2015 Self-healing composites: A review. Cogent Eng 2: 1-28.

WHITE SR, SOTTOS NR, GEUBELLE PH, MOORE JS, KESSLER MR, SRIRAM SR, BROWN EN & VISWANATHAN S. 2001. Autonomic healing of polymer composites. Nature 415: 817-817.

WU DY, MEURE S & SOLOMON D. 2008. Self-healing polymeric materials: a review of recent developments. Prog Polym Sci 33: 479-522.

WU J, WEIR MD, MELO MAS, STRASSLER HE & XU HHK. 2016. Effects of water-aging on self-healing dental composite containing microcapsules. J Dent 47: 86-93.

YANG J, KELLER MW, MOORE JS, WHITE SR & SOTTOS NR. 2008. Microencapsulation of Isocyanates for Self-Healing Polymers Microencapsulation of Isocyanates for Self-Healing Polymers. Macromol 41: 9650-9655.

YANG Y, HE J, LI Q, GAO L, HU J, ZENG R, QIN J, WANG SX & WANG Q. 2019. Self-healing of electrical damage in polymers using superparamagnetic nanoparticles. Nat Nanotechnol 14: 151-155.

YU X, YANG P, ZHANG Z, WANG L, LIU L & WANG Y. 2018. Self-healing polyurethane nanocomposite films with recoverable surface hydrophobicity. J Appl Polym Sci 135: 46421.

ZECHEL S, GEITNER R, ABEND M, SIEGMANN M, ENKE M, KUHL N, KLEIN M, VITZ J, GRÄFE S, DIETZEK B, SCHMITT M, POPP J, SCHUBERT US & HAGER MD. 2017. Intrinsic self-healing polymers with a high E-modulus based on dynamic reversible urea bonds. NPG Asia Mater 9: e420.

ZHAO G, ZHOU Y, WANG J, WU Z, WANG H & CHEN H. 2019. Self-healing of polarizing films via the synergy between gold nanorods and vitrimer. Adv Mater 31: 1900363.

How to cite

CARRARA AE, RODRIGUES VHS, DUTRA RCL & DUTRA JCN. 2023. Impact assessment of synthesis parameter stirring speed in final physicochemical properties of PU microcapsules incorporated into epoxy matrixes. An Acad Bras Cienc 95: e20201518. DOI 10.1590/0001-3765202320201518.

Manuscript received on September 22, 2020;
accepted for publication on February 17, 2021

ALEXANDRE ESTÊVÃO CARRARA
https://orcid.org/0000-0002-6286-1493

VINÍCIUS HENRIQUE DE S. RODRIGUES
https://orcid.org/0000-0003-3798-3170

RITA DE CÁSSIA L. DUTRA
https://orcid.org/0000-0001-9958-1279

JORGE CARLOS N. DUTRA
https://orcid.org/0000-0002-0923-620X

Instituto Tecnológico de Aeronáutica, Departamento de Ciência e Tecnologia Aeroespacial, Praça Marechal Eduardo Gomes, 50, Vila das Acácias, 12228-900 São José dos Campos, SP, Brazil

Correspondence to: **Alexandre Estevão Carrara**
E-mail: alexandre.ecarrara@gmail.com

Author contributions

Conceptualization, Carrara AE, Rodrigues VHS, Dutra JCN; Methodology, Carrara AE, Rodrigues VHS, Dutra JCN, Dutra, RCL; Investigation, Writing – Original Draft Carrara AE; Writing – Review and Editing, Carrara AE, Dutra, JCN, Dutra RCL; Funding Acquisition, Dutra, RCL; Supervision, Dutra JCN.